Scanning Microscopy

Volume 1992
Number 6 *Signal and Image Processing in Microscopy and Microanalysis*

Article 33

1992

The Application of Multispectral Techniques to Analytical Electron Microscopy

P. G. Kenny
University of York

M. Prutton
University of York

R. H. Roberts
Newcastle University

I. R. Barkshire
University of York

J. C. Greenwood
University of York

See next page for additional authors

The Application of Multispectral Techniques to Analytical Electron Microscopy

Authors

P. G. Kenny, M. Prutton, R. H. Roberts, I. R. Barkshire, J. C. Greenwood, M. J. Hadley, and S. P. Tear

Scanning Microscopy Supplement 6, 1992 (pages 361-367) 0892-953X/92$5.00+.00
Scanning Microscopy International, Chicago (AMF O'Hare), IL 60666 USA

THE APPLICATION OF MULTISPECTRAL TECHNIQUES TO ANALYTICAL ELECTRON MICROSCOPY

P.G. Kenny*, M. Prutton, R.H. Roberts†, I.R. Barkshire, J.C. Greenwood, M.J. Hadley and S.P. Tear

Department of Physics, University of York, York, YO1 5DD, U.K.

†Department of Physics, Newcastle University, Newcastle, NSW 2308, Australia.

Abstract

The York multispectral analytical electron microscope (MULSAM) was the first instrument specifically designed to acquire and process multiple Auger, X-ray, backscattered electron, elastically scattered electron, scanning electron microscopy (SEM) and specimen absorption current images simultaneously. Analyzing combinations of these signals with multispectral correlation techniques yields more information than would normally be obtained by treating each image separately. This paper reports some of the multispectral methods we have investigated at York which may be of use to other workers. Included are (1) a method that corrects for beam current fluctuations during long acquisition runs which is based on the anti-correlation between SEM and specimen current images, (2) the classification of topography for crystalline specimens by correlation partitioning of backscattered electron images and (3) the enhancement of surface state contrast in multispectral scanning tunneling microscopy (STM) images using the Hotelling transform. The last example is intended to demonstrate that these techniques can also be applied to other fields in microscopy.

Key Words: multispectral, image processing, electron microscopy, Auger microscopy, scanning tunneling microscopy.

*Address for correspondence:
P.G. Kenny,
Department of Physics,
University of York,
York, YO1 5DD, U.K.
Telephone no: 44 904 432218 (FAX: 432214)

Introduction

Multispectral image analysis techniques exploit correlations between signals collected from more than one source in order to extract more information than would normally be obtained by the conventional approach where each type of image is processed separately. Such methods have been used in the field of remote sensing for many years (Moik, 1980) and are now being applied to scanning transmission electron microscopy (STEM) (Burge et al. 1982), scanning Auger microscopy (Browning, 1985a and 1985b; Prutton et al. 1987), laser microprobe mass spectrometry (Fletcher and Currie, 1987), X-ray photoelectron spectroscopy (XPS) (King et al. 1989), energy dispersive X-ray (EDX) (Bonnet et al. 1991), electron energy loss spectroscopy (EELS) (Bonnet and Trebbia, 1992) and scanning tunneling microscopy (STM, see later).

For multispectral techniques to yield accurate results all images in a set must be registered spatially, ie. corresponding pixels in all images must be sampled from exactly the same point on the specimen. In practice this can only be achieved by collecting all the images in parallel since some specimen drift or vibration is unavoidable during the long acquisition times needed for high quality Auger or EDX images. Parallel acquisition also has the advantage of ensuring that all signals are collected under exactly the same conditions. This may make it possible to extract information about and correct for variations in the conditions. An example of this is given later.

The York multispectral analytical electron microscope (MULSAM, formerly known as a multispectral scanning Auger microscope) was the first instrument specifically designed to acquire and process large multispectral Auger, EDX, backscattered electron (BSE), elastically scattered electron, scanning electron microscopy (SEM) and specimen absorption current images in parallel (Prutton et al. 1990a; Kenny et al. 1989). Since it became operational in late 1990 the MULSAM has been used to investigate and exploit a number of new multispectral techniques (Barkshire et al. 1991a-e; Kenny et al. 1991; Greenwood et al. 1991). This paper describes some of the methods which we think may be of interest to other workers:

(1) Exploitation of the anti-correlation

between SEM and specimen absorption current signals to correct for variations in beam current during long acquisitions.

(2) Classification of the topography of crystalline specimens by correlation partitioning of backscattered electron images.

(3) Use of the Hotelling transform to enhance surface state contrast in multispectral STM images. This example is intended to demonstrate that multispectral techniques can also be applied to other fields in microscopy.

Beam Current Correction Method using Anti-Correlation between SEM and Specimen Current Signals

Beam current variations can be a problem when Auger, EDX or other energy-analyzed images are being collected because of the long acquisition times necessary for accurate results. We have devised a method to correct for such variations which exploits the anti-correlation between SEM and specimen absorption current signals. When an electron beam is scanned across an inhomogeneous surface, a proportion of the incident current will be reflected or re-emitted after some scattering processes and the remainder will be absorbed. The ratio between the total absorbed and total emitted currents will vary with composition, topography etc. but if the specimen is non-insulating and earthed, then the sum of these two currents must always equal the incident beam current. The York MULSAM is equipped with a specimen absorption current detector and the SEM signal is known to be approximately proportional to the total emitted current. It should therefore be possible to estimate beam current from these two signals if the sensitivities and zero-offsets of both detectors are known.

Figures 1(a) and 1(b) show the raw SEM and specimen current images for a sample which consists of a patterned W film on a Si substrate. This was kindly supplied to us by Dr. B. Lamb of Bell Northern Research, Harlow, Essex, U.K. (formerly STL). The beam current was deliberately switched between a number of different settings during acquisition giving rise to horizontal bands in the raw data. Figure 1(d) shows the scatter diagram calculated from these two signals. This is a two dimensional histogram of the intensity distributions for both images with the frequency of occurrence of each combination of intensities represented by brightness (Browning, 1985b; Prutton et al. 1990b). A number of parallel straight lines with bright clusters at each end can be seen. Each line corresponds to a different beam current setting. The end clusters come from the signals on W and Si and the lines joining them come from edges. It can also be seen that the variance due to composition is roughly orthogonal to that due to beam current. This means that the two effects are statistically uncorrelated and it should be possible to separate them by a simple linear combination of the two images.

Figure 1(h) shows an image of the beam current variations which was produced by summing the SEM and specimen current images after each had been normalized to give the same sensitivity to total emitted/absorbed current. Zero-offsets (dark currents) and non-linearities (eg. due to saturation) are corrected automatically by our acquisition system. The relative sensitivity was estimated from the ratio between the ranges of pixel values (ie. maximum - minimum) present in each image. Alternatively, we could have measured the gradient of any one of the parallel bars. Although the latter method should be more accurate it only works if the beam current has been switched in such a way as to produce distinct bars and clusters in the scatter diagram. This will not usually be the case unless an experiment is being performed, such as that presented here, specifically to obtain the relative sensitivity. However, once this factor has been found it may be used to calculate beam current images for new data collected under similar conditions.

Figure 1(h) is clearly dominated by the horizontal bars and the W film pattern has almost vanished, suggesting that it gives a good, but not perfect, measure of the beam current variations. Figures 1(e) and 1(f) show the SEM and specimen current images after they have been divided by 1(h). The horizontal bars have been completely eliminated in these. Figures 1(c) and 1(g) show another image which was collected at the same time, before and after correction. A slight trace of the horizontal bars remains in the corrected image, so beam current variations have not been completely removed in this case. However, this may in part be due to imperfect non-linearity corrections in the original data. It should also be noted that under normal conditions the beam current would not fluctuate by such a large degree.

An important limitation of this technique needs to be mentioned here. Since the SEM detector has a finite collection angle it will not necessarily give a signal which is proportional to the total emitted current if the angular distribution varies much with position. This may be the case with some crystalline specimens. However, any significant departure from the assumed linearity should be revealed in the scatter diagram.

Topography Classification by Correlation Partitioning

It is sometimes desirable to be able to classify the orientations of facets at the surface of a crystalline specimen. The second application presented here shows how this can be carried out interactively using correlation partitioning (Browning, 1985b; Paque et al. 1990) of the signals from a BSE detector.

BSE detectors usually comprise a set of four Si p-n junction quadrants arranged about the axis of the electron gun. They are commonly used to produce images which reveal topographic contrast (Lebiedzik and White, 1975). Figures 2(a) and 2(b) show a pair of images in which horizontal and vertical topographic contrast has been enhanced separately by subtracting images from opposite pairs of detectors in a BSE quadrant. The specimen is a single crystal Si wafer which has been etched anisotropically to produce a number of polyhedra. Only one has been shown here for the sake of clarity. Figure 2(c) is the scatter diagram of the intensity distributions of these two images and consists of several bright clusters

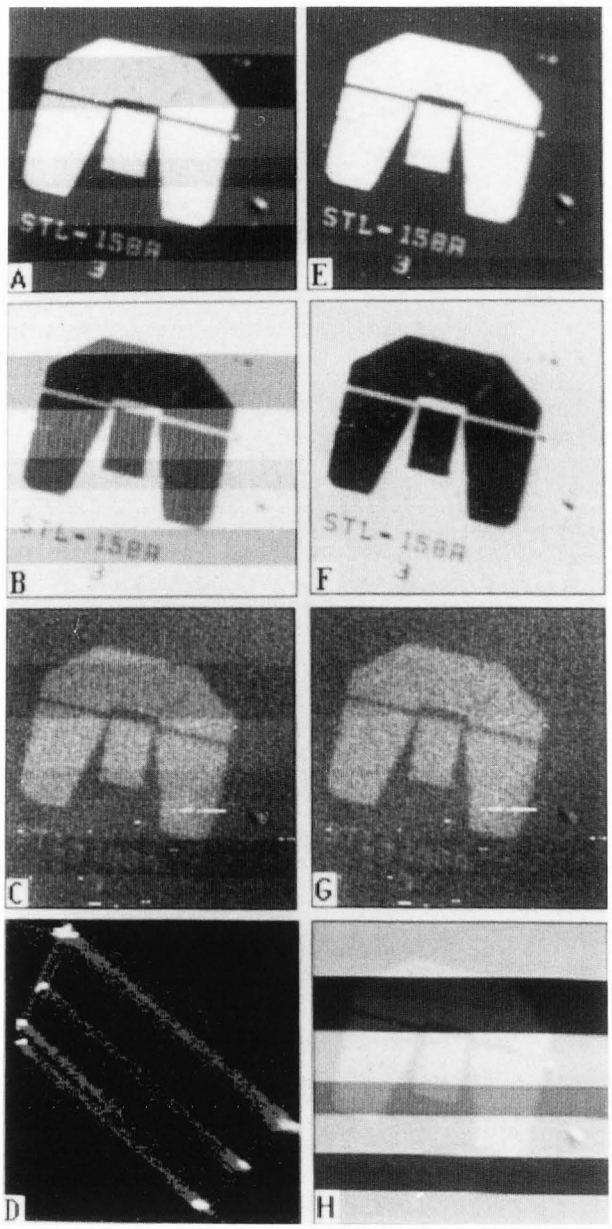

Figure 1. Illustration of the beam current correction method. The sample comprises a patterned W film on a Si substrate and each image is approximately 200μm across. (a), (b) and (c) are the raw SEM, specimen absorption current and 1345eV energy analyzed electron images, respectively. (d) is the scatter diagram of SEM intensity (horizontal) vs specimen current intensity (vertical). (h) is the beam current image estimated from a weighted sum of (a) and (b). (e), (f) and (g) are the corrected SEM, specimen current and 1345eV electron images, respectively.

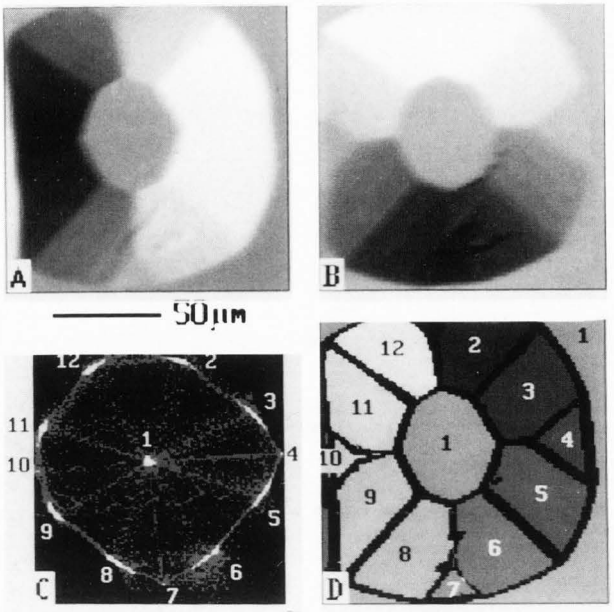

Figure 2. Topography classification by correlation partitioning. The specimen is an anisotropically etched single crystal Si wafer. (a) and (b) are horizontal and vertical topographic contrast images derived from quadrants of a BSE detector. (c) is the scatter diagram of the intensity distributions of (b) vs (a). (d) is a grey scale version of the false color image produced by correlation partitioning. Pixels are colored /shaded according to which cluster they map to in the scatter diagram. Corresponding clusters and facets have been labelled for clarity.

arranged like a wheel. The correlation partitioning technique involves the user drawing windows around features in a scatter diagram from which the computer generates a false color image showing which image pixels map to each such feature. Figure 2(d) is a grey scale representation of a false color image derived by placing a different window around each of the clusters in the scatter diagram. When viewed in color, it is easy to see that each cluster corresponds to a different surface orientation and the lines between adjacent clusters come from the edges between adjacent facets. The grey scale version presented here has been labelled to make the correspondence clearer.

A number of additional points are worth making about the information contained in the scatter diagram 2(c). If the images showed several polyhedra, then the scatter diagram would be identical to the single polyhedron case because the facets would still have the same orientations. This would probably not be the case if they were not etched from a common single crystal wafer. The proportion of the surface with a particular orientation can be determined from the size and brightness of the corresponding cluster. Furthermore, the polar and azimuthal angles could be estimated from the distance and bearing of a cluster relative to the central cluster.

This classification method can be applied to data from more than two images by plotting a separate two dimensional scatter diagram for each unique combination of two images in the set (eg. three scatter diagrams are needed for three images, six for four images etc). A set of bit maps could be generated for each correlation window instead of a false color image. Each bit map could then be used as a mask for some subsequent processing operation. Finally, note that a similar analysis technique has been reported by Tovey et al. (1992).

STM Surface State Enhancement using the Hotelling Transform

For our third example, we have chosen to demonstrate how the Hotelling transform can be applied to multispectral scanning tunneling microscope (STM) data. As far as we are aware, this has not been done before. We hope the results will be sufficiently interesting to encourage others to experiment with this approach.

The Hotelling transform (Moik, 1980; Prutton et al. 1990b) is also known as the principal component, Karhunen-Loéve or eigenvector transform. It is based on a purely statistical analysis of the correlations between corresponding pixels in a multi-image set. Since no physical model is involved, the user need not know how these images are related in advance. If the transform is applied to N partly correlated images then N new images will be produced which are statistically uncorrelated with each other. This has the effect of isolating different signal components which are common to more than one image and can work even if these are too weak to be identified in any of the raw images.

Figures 3(a)-(d) show a representative selection from a multispectral set of 36 images collected on an Omicron Vakuumphysik STM. These were produced by measuring the current (I) at each scan position for a number of sample bias voltages (V). The data was then linearized by calculating (dI/dV)/(I/V) at each pixel and for each sample bias. This is equivalent to d(log(I))/d(log(V)) which is proportional to the density of states (DOS), as explained by Chen (1988). The specimen is a clean Si(111) surface with a 7x7 reconstruction. There appears to be a difference in the contrast and clarity between the upper and lower halves of each image. This may be due to something happening to the tip during the raster scan. The other raw images have not been shown because they would take too much space and in any case look fairly similar.

Figures 3(e)-(l) show the first 8 principal components produced by applying the Hotelling transform to all 36 raw images. These are in order of decreasing significance (ie. eigenvalue) and will be referred to as PCs 1-8. The normalized eigenvalues for these components were respectively 17%, 16%, 12%, 6%, 4%, 3.6%, 3.3% and 3.2%. This means that about 51% of the total information present in all 36 raw images has been shifted into the first 4 components. PC1 and PC2 (e and f) contain nothing but random noise which suggests that two strong and independent sources of noise are present in all or many of the images. PC3 (g) has enhanced the adatom state, although this is not so clear in the upper half. PC4 (h) shows the rest atom dangling bond state and the underlying dimers may just be visible too. Both PC3 and PC4 are significantly less noisy than the raw data. This is expected since a lot of the noise has been shifted into PCs 1 and 2 or the lower order components. PCs 5-7 (i-k) seem to emphasize a number of bright and dark blotches, but with slightly different locations and polarities in each image. These may be due to different kinds of contamination or contamination in different sites. PC8 (l) is interesting because the small dark spots are quite distinct in both halves of the image. The remaining principal components (PCs 9-36) are not shown but are more noisy and do not appear to contain any further useful information.

The Hotelling transform has successfully isolated several important signal components from a large multispectral set. This ability to reduce large data sets to more manageable proportions is a useful property of the transform which can be exploited in several ways. For instance, it would not have been easy to perform interactive correlation partitioning on all 36 raw images as there would be 630 different 2-dimensional scatter diagrams to consider. However, it would be quite easy to apply correlation partitioning to the few significant components which the transform has produced. Furthermore, the resulting false color image could be used as a mask for further applications of the Hotelling transform. Each group of statistically similar regions could thus be analyzed in even greater detail. This approach is known as recursive correlation partitioning (Browning, 1990).

Conclusion

We have tried to demonstrate the value of multispectral techniques in analytical electron microscopy and related fields by presenting three typical applications. When this approach is more widely appreciated we expect equipment manufacturers to begin to design instruments capable of collecting and processing multispectral image data in an more efficient manner.

Acknowledgements

The Authors wish to thank the UK Science and Engineering Research Council (SERC) and Department of Trade and Industry (DTI) for their support of the MULSAM project and for funding this work as part of the "Silicon Towards 2000" initiative. Thanks are also due to Alan Gebbie for photographic work.

References

Barkshire IR, Greenwood JC, Kenny PG, Prutton M, Roberts RH, El Gomati MM. (1991a). Image correlation: application to correction of beam current fluctuations in quantitative surface microscopy. Surface and Interface Analysis 17, 209-212.

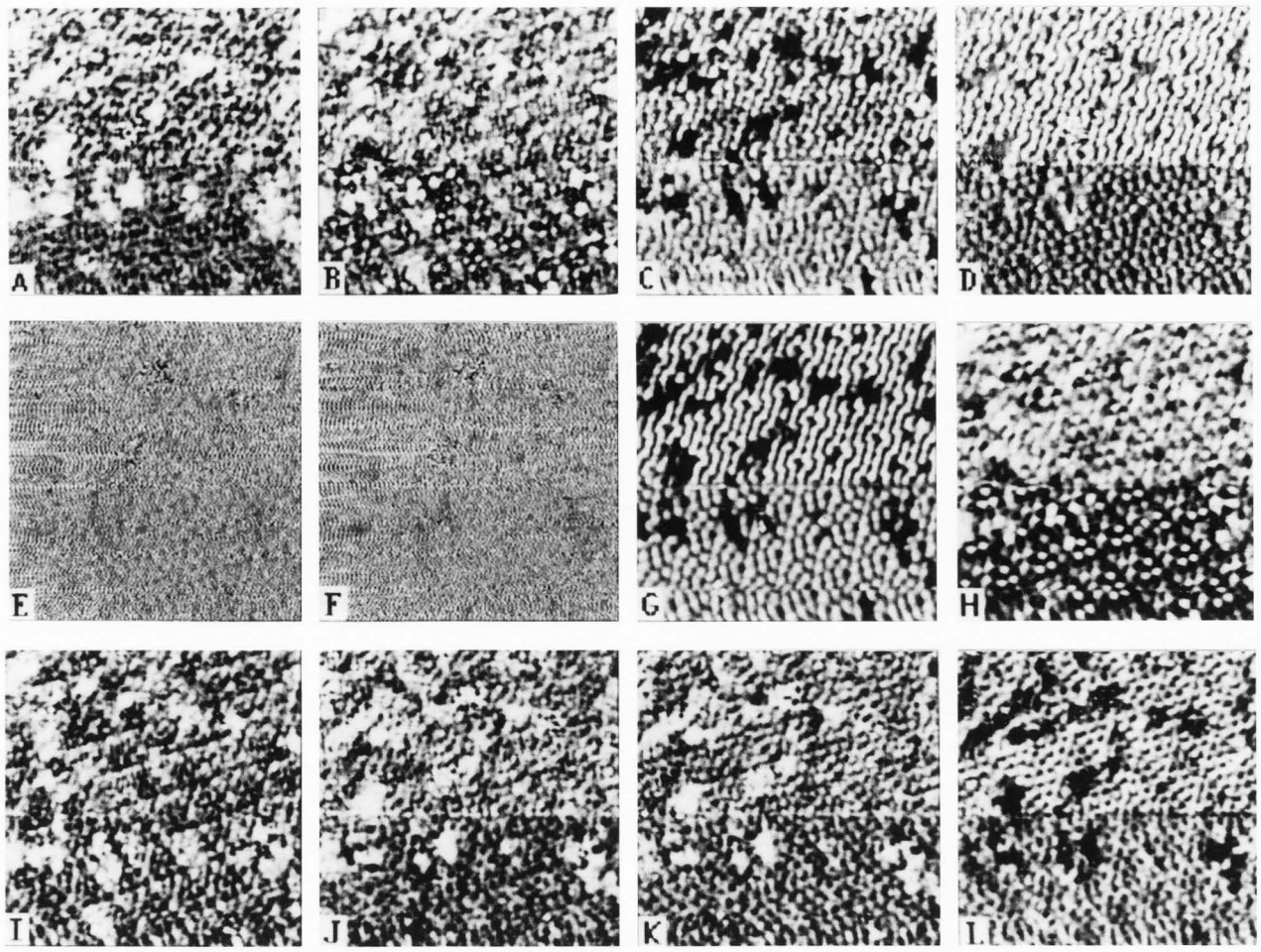

Figure 3. Surface state enhancement of multi-spectral STM "DOS" images (dI/dV)/(I/V) using the Hotelling transform. The sample is a clean Si (111) surface with a 7x7 reconstruction. (a)-(d) are a selection of images representative of a set of 36 for which the sample biases ranged from -1.9V to +1.9V. The biases for those shown were -1.5V, -0.5V, +0.5V and +1.5V respectively. (e)-(l) are the first 8 principal component images produced by applying the Hotelling transform to all 36 raw images and shown in order of decreasing significance (eigenvalue). Note that the bright /dark polarity of these images is arbitrary. See text for interpretation. NB - all of these images apart from (e) and (f) were smoothed using a 25-point fit to a 2D cubic and displayed with their contrast enhanced by histogram equalization. The smoothing was carried out after the Hotelling transform had been applied.

Barkshire IR, El Gomati MM, Greenwood JC, Kenny PG, Prutton M, Roberts RH. (1991b). Topographical contrast using scatter diagrams and correlated images from four backscattered electron detectors. Surface and Interface Analysis 17, 203-208.

Barkshire IR, Prutton M, Skinner DK. (1991c). Correction of backscattering effects in the quantification of Auger depth profiles. Surface and Interface Analysis 17, 213-218.

Barkshire IR, El Gomati MM, Roberts RH, Greenwood JC, Kenny PG. (1991d). Automatic removal of substrate backscattering effects in Auger images. Inst.Phys.Conf.Ser. 119, 185-188 (EMAG 91).

Barkshire IR, Roberts RH, Greenwood JC, Kenny PG. (1991e). Application of ion beam bevel sectioning to semiconducting and metallic layer structures. Inst.Phys.Conf.Ser. 119, 17-20 (EMAG 91).

Bonnet N, Simova E, Thomas X. (1991). Application of multivariate statistical analysis to time dependent spectroscopy. Microsc. Microanal. Microstruct. 2, 129-142.

Bonnet N, Trebbia P. (1992). Multi-dimensional data analysis and processing in electron-induced microanalysis. Scanning Microscopy Supplement 6 (these proceedings).

Browning R. (1985a). Multispectral Auger imaging. Inst.Phys.Conf.Ser. 90, 235-238 (EMAG 85).

Browning R. (1985b). New methods for image collection and analysis in scanning Auger microscopy. J.Vac.Sci.Technol. (A) 3, 1959-1964.

Browning R, King PL, Paque JM, Pianetta P. (1990). EDX image classification by recursive partitioning, in: Microbeam analysis 1990, J.R. Michael and P. Ingram (ed), San Francisco Press, 199-202.

Burge RE, Browne MT, Charalambous P, Clarke A, Wu JK. (1982). Multiple images in STEM. Journal of Microscopy 127, 47-60.

Chen C Julian. (1988). Theory of scanning tunneling spectroscopy. J.Vac.Sci.Technol. (A) 6, 319-322.

Fletcher RA, Currie LA. (1987). Observations derived from the application of principal component analysis to laser microprobe mass spectrometry, in: Microbeam analysis 1987, R.H. Geiss (ed), San Francisco Press, 369-371.

Greenwood JC, Skinner DK, Prutton M. (1991). The use of substrate thinning to enhance the detectability of elements in Auger spectroscopy and imaging. Inst.Phys.Conf.Ser. 119, 25-28 (EMAG 91).

Kenny PG, Prutton M, El Gomati MM. (1989). The implementation of multispectral Auger microscopy. Inst.Phys.Conf.Ser. 98, 295-298 (EMAG-MICRO 89).

Kenny PG, Prutton M, Barkshire IR, Greenwood JC, Roberts RH. (1991). The acquisition and processing of multispectral analytical electron microscope images. Inst.Phys.Conf.Ser. 119, 29-32 (EMAG 91).

King PL, Browning R, Pianetta P, Lindau I, Keenlyside M, Knapp G. (1989). Image processing of multispectral X-ray photoelectron spectroscopy images. J.Vac.Sci.Technol (A) 7 3301-3305.

Lebiedzik J, White EW. (1975). Multiple detector method for the quantitative determination of microtopography in the SEM. Scanning Electron Microsc. 1975; I: 181-188.

Moik JG. (1980). Digital processing of remotely sensed images. NASA SP-431, U.S. Government Printing Office, Washington D.C. Chapter 8.

Paque JM, Browning R, King PL, Pianetta P. (1990). Quantitative information from X-ray images of geological materials, in: Microbeam Analysis 1990, J.R. Michael and P. Ingram (ed), San Francisco Press, 195-198.

Prutton M, El Gomati MM, Walker CGH. (1987). Quantitative imaging in the scanning Auger microscope. Inst.Phys.Conf.Ser. 90, 1-8 (EMAG 87).

Prutton M, Walker CGH, Greenwood JC, Kenny PG, Dee JC, Barkshire IR, Roberts RH, El Gomati MM. (1990a). A third generation Auger microscope using parallel multispectral data acquisition and analysis. Surface and interface analysis 17, 71-84.

Prutton M, El Gomati MM, Kenny PG. (1990b). Scatter diagrams and Hotelling transforms: application to surface analytical microscopy. J.Elect.Spect. and R.P. 52, 197-219.

Tovey NK, Smart P, Hounslow MW. (1992). Automatic orientation analysis of microfabric. Scanning Microscopy Supplement 6, 315-330.

Discussion with Reviewers

R.Browning: A question about names. Should we really call this multispectral imaging? We are now using the SEM, sample current and backscattered counts which are not normally considered to be spectral signals. As multi-channel has another specific meaning would multivariate or multi-dimensional be better nomenclature?

Authors: The term "multispectral" was inherited from the earlier application of these methods to multispectral satellite images and we agree that it has become too narrow. Although "multivariate" and "multi-dimensional" are more general they lack the sense of there being a physical property involved. Perhaps the new approach could be called "multivariate microanalysis"?

R.Browning: The additional contrast due to the W pattern in figure 1h suggests that the SEM detector is not sampling other currents, such as the backscattered electron distribution, particularly well. Would it be better to include the backscattering current in the current normalization scheme through a three dimensional histogram?

Authors: If a more accurate measure of beam current is needed then more signals, such as the BSE, may be included in the calculation. In our experience, applying the Hotelling transform to all suitable images in a set usually produces a component which reveals beam current variations. The corresponding eigenvector coefficients may provide a starting point for a more sophisticated calculation, but we have not pursued this.

R.Browning: The use of multispectral techniques for the analysis of STM images is a very interesting development. Can you partition the multivariate histogram from the Si image and thus produce spectra for each of the partitioned areas, or is there no clear clustering within this histogram?

Authors: The scatter diagram clusters overlapped but it was just possible to partition the different sites. Some spectroscopic information has been extracted by a different method, see the next question.

N.Bonnet: We know that STM image sequences are difficult to interpret and therefore I approve of trying to identify the different "sources of information" by using the Hotelling transform (or principal component analysis). This first trial has given encouraging results. However, some of these results are also disappointing, in particular the fact that the first two factorial axes represent noise.

In this kind of analysis the factorial axes may also be interpreted by plotting the weights of the different images for the main principal components (dual representation). Did you observe significant interpretable features with this representation?

Authors: Plotting the weights (eigenvector coefficients) as a function of sample bias did yield some spectroscopic information. For PC3, the adatom state, there were two peaks at about

+0.4V and +1.1V. For PC4, the rest atom dangling bond state, there was a single sharp peak at -0.6V. These correspond to potentials where the density of states is expected to change most rapidly for the sites identified by these components.

N. Bonnet: As the authors suggest, it seems that the STM data is corrupted by something happening to the tip during the raster scan. May this be the reason why the results are difficult to interpret? I would suggest that principal component analysis be performed on the upper half of the data set only and the results compared.
Authors: The results could probably be simplified by choosing to analyze a smaller region within the original raster area, but this defeats part of the purpose of the experiment which was to demonstrate how the Hotelling transform can extract useful information from complex data. As far as we are aware, STM data has never been subjected to this kind of analysis before. A more rigorous analysis of better data will be the subject of future work.

R. E. Burge: In respect of the application of the Karhunen-Loéve (Hotelling) transform to the multispectral data, a comment would be valuable on the reason for the very high level of 33% of information in the data set which is said to be due to random noise. This high noise content does not seem to be present in the images shown (figures 3a-d). What criteria were used to accept each additional image into the K-L set and how many were mainly records of noise?
Authors: As stated in the caption to figure 3, all images apart from (e) and (f) were smoothed prior to display (but after the Hotelling transform had been applied). The raw data was in fact very noisy. Only one or two of the 36 images included in the calculation were dominated by random noise. We did exclude images for which the magnitude of the sample bias was less than 0.2V because these appeared to contain nothing but noise.

R. E. Burge: It is said that the two primary principal component images are due to independent noise. The inference is that the cross-correlation between the two fields (e) and (f) in figure 3 is zero. The similarity between the images indicates that the cross-correlation is unlikely to be zero. Perhaps the authors will calculate the cross-correlation and comment.
Authors: The apparent similarity between the noise components (e) and (f) is intriguing but deceptive. If you look more closely and compare them pixel by pixel, you will see they are actually quite different. The cross-correlation is indeed zero and plotting a scatter diagram reveals a radially symmetric Gaussian-like distribution centered on the intensity origin. The apparent similarity may be due to the presence of a common noise component which affected the scan position (scan noise).

R. E. Burge: A comment would be helpful as to how different in image representation a set of images may be for the assumption to be made that they can form a K-L set. Indeed, might it be that the high noise content arises because this set of images is not a satisfactory one for the application of the method?
Authors: As long as the images are spatially registered, contain some information and are not dominated by non-linear contrast effects there seems no point in excluding anything from the Hotelling transform, at least initially. Including noisy data does not usually cause problems because the transform (as applied here) is based on the correlation matrix which is relatively insensitive to purely random noise. As indicated in the text, the reason why the two most significant principal components show noise is because the noise in the different images must be strongly correlated. This was not apparent in the raw (unsmoothed) data and so we have learned something interesting. Indeed, the Hotelling transform has revealed quite a lot of interesting information about our STM data, so we consider its application to have been successful.